II. MICROWAVE GASEOUS DISCHARGES*

Prof. S. C. Brown
Prof. W. P. Allis
Prof. D. J. Rose
Prof. D. R. Whitehouse
Dr. G. Bekefi
Dr. L. Mower
C. D. Buntschuh
J. D. Coccoli
S. Frankenthal
R. B. Hall
R. L. Hall
J. L. Hirshfield
W. R. Kittredge
J. J. McCarthy
W. J. Mulligan
G. B. Nichols
Judith L. Shaver
C. S. Ward

A. ACCELERATION OF A NEUTRALIZED ION BEAM

A class of velocity distributions exists which permits acceleration of one type of particle in a dc electric field, without any space-charge effects. Consider, for example, the diagram of Fig. II-1, and the acceleration of an ion beam. The ions travel to the

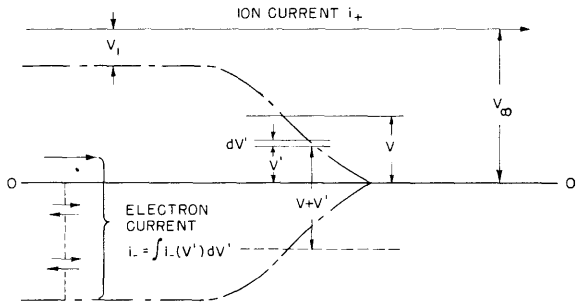

Fig. II-1. Voltages and currents in space-charge-free sheath.

right, and have final energy V_∞ (electron-volts) in the region at the right of the figure; the potential of that region is conveniently set equal to zero. To the left, there is an uphill region for ions, and its mirror image for electrons. Finally, the ions came from a region where they had energy V_1, and thus they were accelerated through the difference $V_\infty - V_1$.

Now let there be an electron current di_- at an energy V' relative to zero in the energy interval dV'. At some place where the potential is V, the velocity of such an electron is

$$\left[\frac{2e(V'+V)}{m_-}\right]^{1/2}$$

and the contribution dn_- to the electron density n_- is

*This work was supported in part by the Atomic Energy Commission under Contract AT(30-1)-1842.

$$dn_- = \frac{i_-(V')\,dV'}{e\left[\frac{2e(V'+V)}{m_-}\right]^{1/2}} \tag{1}$$

We must now integrate over all contributions, and set the density equal to that of the ions of mass m_+ in the beam i_+. In this example, electrons incident from the left with energy less than zero are reflected, and their contribution must be counted twice. Thus, after cross-multiplying, we have

$$i_+\left(\frac{m_+}{m_-(V_\infty - V)}\right)^{1/2} = \int_0^\infty \frac{i_-(V')\,dV'}{(V'+V)^{1/2}} + 2\int_{-V}^0 \frac{i_-(V')\,dV'}{(V'+V)^{1/2}} \tag{2}$$

as the defining equation for $i_-(V)$.

Any reasonable function can be chosen for $i_-(V')$ in the energy range $V' > 0$, as long as neutrality is achieved on the right of Fig. II-1. Suppose again, for example, that a beam i_2 of electrons at final energy V_2 provides this neutralization. The first integral of Eq. 2 is trivial. If we set

$$E = -V' \tag{3}$$

for convenience (electron energy measured as positive down from zero), we obtain

$$\int_0^V \frac{i_-(E)\,dE}{(V-E)^{1/2}} = \frac{i_+}{2}\left(\frac{m_+}{m_-}\right)^{1/2}\left[\frac{1}{(V_\infty - V)^{1/2}} - \left(\frac{V_2}{V_\infty(V_1+V)}\right)^{1/2}\right] \tag{4}$$

This is a Volterra equation of the first kind whose solution is

$$i_-(V) = \frac{i_+}{2\pi}\left(\frac{m_+}{m_-}\right)^{1/2}\left[\left(\frac{V_\infty}{V}\right)^{1/2}\frac{1}{(V_\infty - V)} - \frac{1}{(VV_\infty)^{1/2}(1+V/V_2)}\right] \tag{5}$$

We can find the total electron current ($\approx i_+(m_+/m_-)^{1/2}$ or greater) by integrating $i_-(V)$ over all contributions. We can also take other suitable functions for the electron distribution at positive energy.

Since no space charge arises, the concept is applicable to a beam of any lateral dimension.

D. J. Rose

B. MICROWAVE NOISE RADIATION FROM PLASMAS

Previously, we reported (1) measurements of the microwave noise from a plasma column radiating into a waveguide. The results were compared with calculations based on a geometrical-optics model for the transfer of radiation from within the body

of the plasma. In this model, scattering from the boundaries of the plasma was neglected. This neglect may lead to a considerable error whenever boundary effects become important, as, for instance, with very dense plasmas (i.e., high electron concentration).

A general formulation of the theory, free from these objections, has been obtained with the aid of Nyquist's theorem (2, 3). The low-frequency noise power P per unit frequency interval received from a body at a temperature T is

$$P = kT \cdot A \tag{1}$$

Here A represents the absorption coefficient of the plasma, defined as that fraction of the total incident power absorbed by the plasma from a test wave launched from the position of the noise detector. If more than one mode can propagate down the guide within the given frequency interval, A represents the sum of the absorption coefficients of all the modes.

Let $\vec{E}_i$ and $\vec{H}_i$ be the field components of the incident test wave, $\vec{E}$ the field within the absorbing plasma of electric conductivity σ, and $\vec{J}$ the current density. Then

$$A = \int_{\text{plasma}} \operatorname{Re}\left(\overline{\frac{1}{2}\vec{E} \cdot \vec{J}^*}\right) dv \Big/ \int_{\text{waveguide}} \operatorname{Re}\left(\overline{\frac{1}{2}\vec{E}_i \times \vec{H}_i^*}\right) da \tag{2}$$

with $\vec{J} = \sigma\vec{E}$. The integration in the numerator of Eq. 2 is carried out over the volume of the plasma; the integration in the denominator is over the waveguide cross-section area. The evaluation of A from Eq. 2 is a boundary-value problem that is amenable to solution in a limited number of cases. One such case is for a low-electron-density plasma of arbitrary shape and of arbitrary electron-density distribution. When the ratio of plasma frequency to radian frequency is small, the incident test wave is perturbed very slightly, so that $\vec{E} \approx \vec{E}_i$ and $\vec{J} \approx \sigma\vec{E}_i$. The results for A thus obtained, and hence the magnitude of the noise power P found from Eq. 1, are identical with those found from the geometrical-optics model that was discussed previously (1).

Numerical computations of A for other than weakly ionized plasmas are being made for a uniform-plasma slab that completely fills the cross section of a rectangular waveguide, and for a uniform-plasma cylinder (4). These computations for various plasma parameters are being made with the view of establishing the limitations of the geometrical-optics approach.

Despite the difficulties of finding the absorption coefficient corresponding to our experimental arrangement (nonuniform-plasma cylinder traversing a rectangular guide), A is amenable to direct measurement. In terms of the reflection and transmission coefficients Γ and T, A is given by

$$A = 1 - |\Gamma|^2 - |T|^2 \tag{3}$$

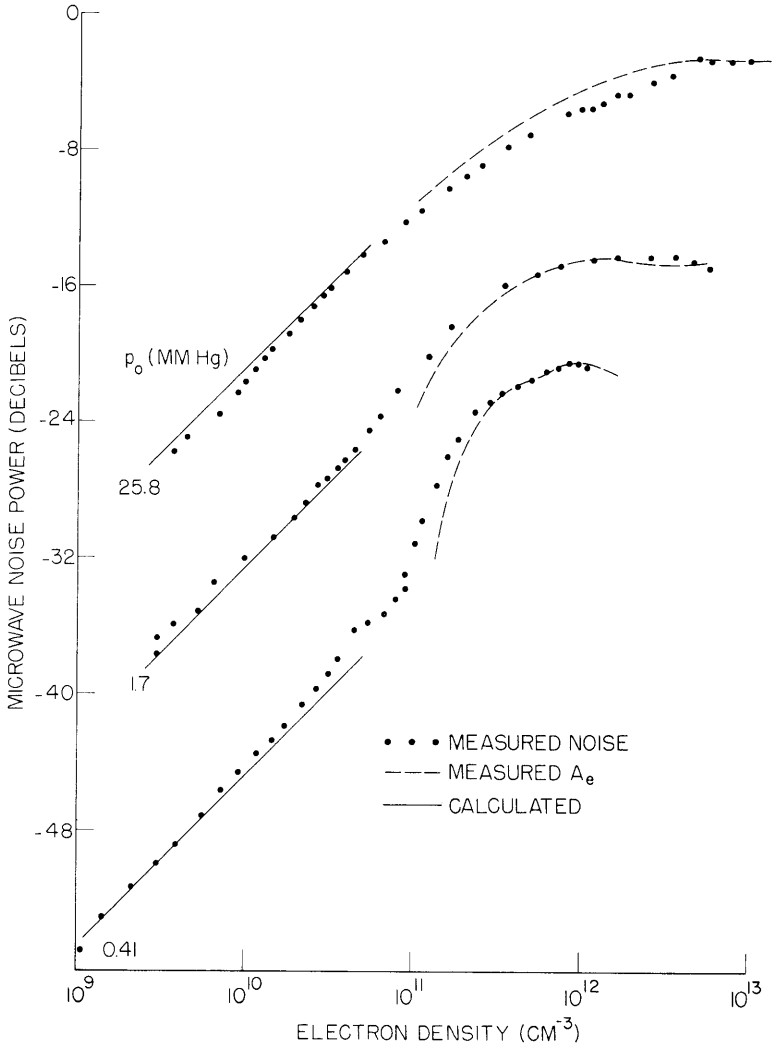

Fig. II-2. Microwave noise power as a function of electron density.

The test wave should be bandlimited noise with a bandwidth equal to that of the radiometer (2 mc). However, in our measurements of A, a monochromatic source set at the center of the frequency band (3000 mc) was used.

Figure II-2 shows a comparison between measurement and theory for a helium plasma at gas pressures of 25.8, 1.7, and 0.41 mm Hg. The solid dots represent noise-power measurements in decibels below the maximum as a function of electron density. These noise-power measurements are corrected for reflections from the plasma (1). The solid straight lines are computed from Eqs. 1 and 2 for the limiting case of a tenuous plasma and should, therefore, agree with the noise measurements in the limit of low electron densities. The dashed lines indicate results obtained from data of the transmission and reflection coefficients of the plasma, as a function of electron

density. Specifically, it is a plot of A_e related to A through

$$A_e = A/(1 - |\Gamma|^2)$$

The effective absorption coefficient, A_e, can be defined as the fraction of the available power absorbed from the test wave after removal of the gross effects resulting from reflections from the plasma. When A_e is unity, $P = (1 - |\Gamma|^2)kT$, and the radiating plasma may then be looked upon as a "black body" mismatched to its surroundings. Measurements for the three gas pressures of Fig. II-2 have shown that the maximum value of A_e lies between 0.86 and 0.89.

The measurements of A_e agree fairly satisfactorily with the noise measurements. The accuracy in the determination of A_e is governed by the precision in finding Γ and T, which, in turn, is chiefly governed by the accuracy of the available precision attenuators. These have been calibrated with an accuracy of ±0.5 per cent. If, for instance, $A_e \leq 0.1$, the error in A_e can exceed ±90 per cent.

G. Bekefi, J. L. Hirshfield

References

1. G. Bekefi and J. L. Hirshfield, Microwave noise radiation from plasmas, Quarterly Progress Report No. 52, Research Laboratory of Electronics, M.I.T., Jan. 15, 1959, pp. 6-12.

2. S. M. Rytov, Theory of Electrical Fluctuations and Thermal Radiation (Izd-vo Akademiia Nauk S.S.S.R., Moscow, 1953).

3. M. L. Levin, J.E.T.P. (Soviet Physics) 4, 225 (1957); Dokl. Akad. Nauk (S.S.S.R.) 102, 53 (1955).

4. N. Marcuvitz, Waveguide Handbook, Radiation Laboratory Series, Vol. 10 (McGraw-Hill Book Company, New York, 1951).

C. ANOMALOUS CONSTRICTION IN LOW-PRESSURE MICROWAVE DISCHARGES IN HYDROGEN

In the course of experiments on low-pressure microwave plasmas a discharge constriction was observed. The experimental apparatus that was used may be described as follows.

A discharge tube, 1 cm in diameter, filled with hydrogen at 1-5 μ Hg pressure, is mounted coaxially inside a cylindrical cavity, 10 cm in diameter, placed between the pole faces of an electromagnet. This magnet furnishes a longitudinal dc magnetic field whose strength can be varied between zero and approximately 1200 gauss. The empty cavity resonates in the TE_{111} mode at S-band and is probe-coupled to a microwave line that is fed by a 50-watt magnetron. A discharge occurs through cyclotron resonance. The TM_{020} mode at C-band is also used as a probing mode to

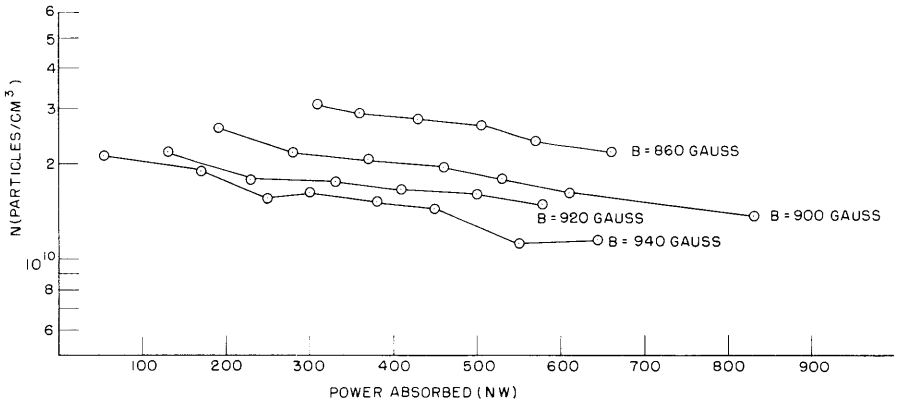

Fig. II-3. Electron density versus power absorbed.

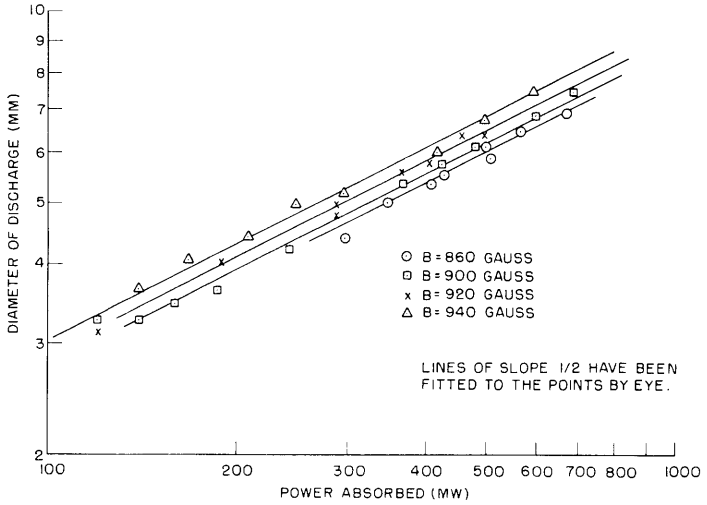

Fig. II-4. Discharge diameter versus power absorbed.

measure average electron densities.

For absorbed powers greater than approximately 900 mw the discharge completely fills the discharge tube. Decreasing the absorbed power below this figure causes the discharge to pull away from the side walls and to continuously decrease in diameter until the absorbed power is so low that the discharge can no longer be maintained. The smallest diameters observed in this manner were approximately 1.5 mm at absorbed powers between 20 and 50 mw. This lower limit varied somewhat with applied magnetic field.

Figures II-3 and II-4 show the electron density and discharge diameter as a function of absorbed power for different magnetic fields. Note that the electron density remains essentially constant for any given magnetic field. The values shown were obtained by

normalizing the data on frequency shifts of the TM_{020} mode to the visible diameter of the discharge. As would be expected from the observation of constant electron density, Fig. II-4 shows that the absorbed power is directly proportional to the discharge volume.

Notice also that average electron density decreases, whereas the discharge volume increases with increasing magnetic field. Hence, for any given absorbed power, the discharge becomes more tenuous as the magnetic field is increased.

The search for a mechanism to explain the cause of the constriction continues.

C. S. Ward

D. CONSTRUCTION OF A MAGNETIC MIRROR

A theoretical design of a mirror magnetic field was presented in a previous report (1). The objective of the design was to generate a magnetic mirror having a hill ratio of approximately 5:1 and possessing a field of 1000 gauss, with a uniformity of 0.5 per cent, over a central cylindrical region of 6-cm length and 2-cm radius.

The design was achieved by selecting the following solution of Laplace's equation in cylindrical coordinates:

$$\vec{B} = \nabla\phi = Ak \{\vec{a}_r[J_1(kr) \sinh(kz) - I_1(kr) \sin(kz)]$$

$$- \vec{a}_z[J_o(kr) \cosh(kz) + I_o(kr) \cos(kz)]\}$$

This magnetic field satisfies the uniformity requirements in the central region and rises rapidly along the axis farther away from the center.

The shapes of the constant flux contours and of the equipotentials associated with this solution were calculated. The desired field can be generated by placing an azimuthal current sheath along a constant-flux contour, with a surface-current density.

$$J_\theta = \frac{1}{\mu_o} B_z$$

where B_z is evaluated along the contour, and by terminating the unit with equipotential boundaries. (See Fig. II-5.)

Aside from the fact that it provides a field with a known, and relatively simple, analytical expression, this unit will be more economical of power than one consisting of a conventional solenoid equipped with more turns at the end than at the center, since the increase of magnetic field is partly achieved by a reduction of the diameter of the turns at the end, rather than by an increase in magnetomotive force.

The unit is to be operated at a high current (2000 amp) and low voltage (4 volts). This should result in a low inductance, and make the unit easier to operate in a pulsed fashion.

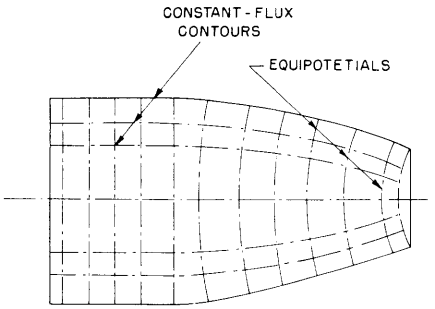

Fig. II-5. Equipotentials and constant-flux contours in the mirror magnetic field.

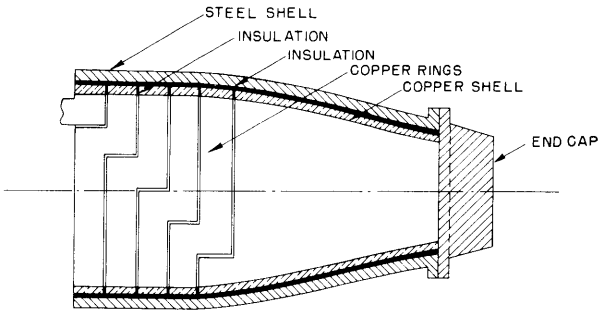

Fig. II-6. Mechanical structure of the mirror magnet.

1. Construction

The current sheath was simulated by a series of coaxial cylindrical rings, of diminishing diameters and cross sections, forming a copper shell whose shape resembles that of a constant flux contour. To insure the accuracy of the generated field, the H-field outside the copper shell was forced to vanish by enclosing the copper shell in a steel shell. Steel end caps provided equipotential boundaries at the ends. (See Fig. II-6.)

The unit was constructed in two halves, each of which was mounted on a rolling carriage, to permit the installation of equipment. Four access ports were drilled around the central rings.

Initial attempts to electroform the copper shell were not successful. As a result, each copper ring had to be manufactured and shaped individually. Insulation between rings consisted of 2-mil P-18 material, and the joints were soft-soldered. Hydrogen brazing was impossible because of impurities in the copper. Mechanical joints were considered, but the problems associated with designing and constructing them (especially for the smaller rings) were sufficiently complex to warrant the selection of soft-soldering.

The magnetic shells were made of low-carbon steel. The specifications called for machining them to fit the shape of the outside surface of the copper shell, leaving a 1-mil gap for a sprayed layer of insulation (Teflon). (The thickness of the gap is

critical because it impedes the heat transfer from copper to steel.) This specification was not met. Gaps of 20 mils were found and had to be filled with epoxy resin.

The end caps were constructed of low-carbon steel; 1-cm access ports were drilled in the center of each. Current was supplied to the copper shell by means of a bolt passing through each end cap.

Cooling was achieved by water-carrying copper tubing wound around the outside of the steel shell.

2. Operation

The magnetic field was tested with a 600-amp current flowing through the unit. At this level, the field was 320 gauss at the center and 1350 gauss at the ends.

Because of inefficient cooling, the magnet could not be operated at a 2000-amp level. At that level, the copper temperature rose to 125° C, and the expansion of the rings, although it was partly limited, stressed and broke the joints between them.

3. Evaluation

The magnetic field configuration provided by the unit is satisfactory. Its failure resulted from weakness in the structure of the copper shell (soft-solder joints) and inefficient cooling. The mechanical weakness could probably be tolerated if the cooling were more efficient. It is evident, however, that with 20-mil gaps between the copper and steel shells, the heat dissipated (8 kw) cannot be carried away efficiently.

The present unit can be rendered operational if the copper shell is cooled by water flowing directly on its inside surface. This modification is under construction. This will require the drilling of additional access ports for the copper tubing, and will make disassembly of the unit difficult. This undesirable feature is, however, a necessary evil. It may also be advisable to consider strengthening the structure of the copper shell by using mechanical or hard-soldered joints between the rings.

S. Frankenthal

References

1. D. C. White, Inhomogeneous magnetic-field design, Quarterly Progress Report, Research Laboratory of Electronics, M.I.T., July 15, 1957, p. 16.